

Global investigation of odd-even mass differences and radii with isospin dependent pairing interactions

C. A. Bertulani,¹ Hongliang Liu,¹ and H. Sagawa²

¹*Department of Physics, Texas A&M University-Commerce, Commerce, Texas 75429, USA*

²*Center for Mathematics and Physics, University of Aizu, Aizu-Wakamatsu, 965-8580 Fukushima, Japan*

(Dated: November 11, 2018)

The neutron and proton odd-even mass differences are systematically studied with Hartree-Fock+BCS (HFBCS) calculations with Skyrme interactions and an isospin dependent contact pairing interaction. The strength of pairing interactions is determined to reproduce empirical odd-even mass differences in a wide region of mass table. By using the optimal parameter, we perform global HF+BCS calculations of nuclei and compare with experimental data. The importance of isospin dependence of the pairing interaction is singled out for odd-even mass differences in medium and heavy isotopes. The proton and neutron radii are studied systematically by using the same model.

PACS numbers: 21.30.Fe, 21.60.-n

Keywords: effective pairing interaction, isospin dependence, finite nuclei

I. INTRODUCTION

Microscopic theories for calculating nuclear masses and/or binding energies (see, e.g., [1–3]), have been revived and further elaborated with the advance of computational resources. These advances are now sufficient to perform global studies based on, e.g., self-consistent mean field theory, sometimes also denoted by density functional theory (DFT) [4, 5]. One particular aspect of the nuclear binding problem is a phenomenon of odd-even staggering (OES) of the binding energy. Numerous microscopic calculations have been published that treat individual isotope chains. However, it might be necessary to examine the whole body of OES data to draw general conclusions [6].

Theoretically, OES values are often inferred from the average HFBCS or Hartree-Fock-Bogoliubov gaps [7–9], rather than directly calculated from the experimental binding energy differences between even and odd nuclei. It should be mentioned that the average HFB gaps are sometimes substantially different from the odd-even mass differences calculated from experimental binding energies. In this work, we compare directly the calculated OES with the ones extracted from experiment. One should say that there are also several prescriptions to obtain the OES from experiments, such as 3-point, 4-point, and 5-point formulas [6]. We adopt the 3-point formula $\Delta^{(3)}$ centered at an odd nucleus, i.e., odd- N nucleus for neutron gap and odd- Z nucleus for proton gap [2]:

$$\Delta^{(3)}(N, Z) \equiv \frac{\pi_{A+1}}{2} \left[B(N-1, Z) - 2B(N, Z) + B(N+1, Z) \right], \quad (1)$$

where $B(N, Z)$ is the binding energy of (N, Z) nucleus and $\pi_A = (-)^A$ is the number parity with $A = N + Z$.

For even nuclei, the OES is known to be sensitive not only to the pairing gap, but also to mean field effects, i.e., shell effects and deformations [6, 7]. Therefore, the comparison of a theoretical pairing gap with OES should

be done with some discretion. One advantage of $\Delta_o^{(3)}$ ($N = \text{odd}$ in Eq. (1)) is the suppression of the contributions from the mean field to the gap energy. Another advantage of $\Delta_o^{(3)}(N, Z)$ is that it can be applied to more experimental mass data than the higher order OES formulas. At a shell closure, the OES (Eq. (1)) does not go to zero as expected, but it increases substantially. This large gap is an artifact due to the shell effect, which is totally independent of the pairing gap itself.

Recently, an effective isospin dependent pairing interaction was proposed from the study of nuclear matter pairing gaps calculated by realistic nucleon-nucleon interactions. In Ref. [8], the density-dependent pairing interaction was defined as

$$V_{pair}(1, 2) = V_0 g_\tau[\rho, \beta\tau_z] \delta(\mathbf{r}_1 - \mathbf{r}_2), \quad (2)$$

where $\rho = \rho_n + \rho_p$ is the nuclear density and β is the asymmetry parameter $\beta = (\rho_n - \rho_p)/\rho$. The isovector dependence is introduced through the density-dependent term g_τ . The function g_τ is determined by the pairing gaps in nuclear matter and its functional form is given by

$$g_\tau[\rho, \beta\tau_z] = 1 - f_s(\beta\tau_z)\eta_s \left(\frac{\rho}{\rho_0}\right)^{\alpha_s} - f_n(\beta\tau_z)\eta_n \left(\frac{\rho}{\rho_0}\right)^{\alpha_n}, \quad (3)$$

where $\rho_0 = 0.16 \text{ fm}^{-3}$ is the saturation density of symmetric nuclear matter. We choose $f_s(\beta\tau_z) = 1 - f_n(\beta\tau_z)$ and $f_n(\beta\tau_z) = \beta\tau_z = [\rho_n(\mathbf{r}) - \rho_p(\mathbf{r})]\tau_z/\rho(\mathbf{r})$. The parameters for g_τ are obtained from the fit to the pairing gaps in symmetric and neutron matter obtained by the microscopic nucleon-nucleon interaction.

In the literature and in many mean field codes publicly available such as the original EV8 code [10], a pure contact interaction is used without an isospin dependence. In our notation, this amounts replacing the isospin dependent function g_τ in Eq. (2) by the isoscalar function

$$g_s = 1 - \eta_s \left(\frac{\rho}{\rho_0}\right)^{\alpha_s}. \quad (4)$$

TABLE I: Parameters for the density-dependent function g_τ defined in Eqs. (2) and (3) for the IS+IV interaction (first row) and g_s in Eq. (4) for the IS interaction. The parameters for g_τ are obtained from the fit to the pairing gaps in symmetric and neutron matter obtained with the microscopic nucleon-nucleon interaction. The pairing strength V_0 is adjusted to give the best fit to odd-even staggering of nuclear masses. The parameters for g_s correspond to a surface peaked pairing interaction with no isospin dependence.

interaction	V_0 (MeVfm ³)	ρ_0 (fm ⁻³)	η_s	α_s	η_n	α_n
g_τ (isotopes)	1040	0.16	0.677	0.365	0.931	0.378
g_τ (isotones)	1120	0.16	0.677	0.365	0.931	0.378
g_s (isotopes)	1300	0.16	1.	1.	—	—
g_s (isotones)	1500	0.16	1.	1.	—	—

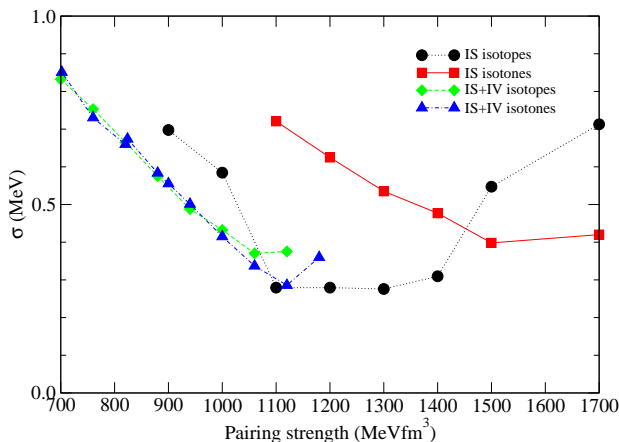


FIG. 1: (Color online) The mean square deviation σ of OES between experimental data and the HF+BCS calculations. The filled circles and squares correspond to the results with IS pairing for neutron and proton gaps, respectively, while the filled diamonds and triangles are those of IS+IV pairing for neutron and proton gaps. Experimental data are taken from Ref. [17]. See the text for details.

The EV8 code has been modified, using the filling approximation, to account for mass calculations for odd-N and odd-Z nuclei and is publicly available as the EV8odd code [11]. It has also been modified to include isospin dependent pairing, by means of Eq. (2). The parameters of the isoscalar interaction were adjusted with EV8 to a best global fit of nuclear masses [12]. They correspond to a surface peaked pairing interaction (Eq. (4) with η_s not too far from the unity).

A recent publication has explored the isospin dependence of the pairing force for the OES effect for a few selected isotopic and isotonic chains [13]. Here we have made a more ambitious study by extending the calculation to the whole nuclear chart. We have also explored

several other observables such as neutron and proton radii systematically which may allow for more solid conclusions on isospin dependent pairing interactions.

This paper is organized as follows. In section II we discuss our numerical calculation strategy. Our results are presented in section III for the energies, separation energies, OES energies, and nuclear radii. Our conclusions are presented in section IV.

II. CALCULATION STRATEGY

The HF+BCS calculations are performed by using SLy4 Skyrme interaction which was found to be the most accurate interaction for studying OES for a few selected ($N = 50, 82$) isotonic and (Sn and Pb) isotopic chains [13]. Our iteration procedure used in connection to EV8odd achieves an accuracy of about 100 keV, or less, with 500 Hartree-Fock iterations for each nuclear state. Our calculations were performed with the now decommissioned XT4 Jaguar supercomputer at ORNL, as part of the UNEDF-SciDAC-2 collaboration [14].

The HF+BCS calculations were first performed for even-even nuclei. The variables in the theory are the orbital wave functions ϕ_i and the BCS amplitudes v_i and $u_i = \sqrt{1 - v_i^2}$. By solving the BCS equations for the amplitudes, one obtains the pairing energy from

$$E_{pair} = \sum_{i \neq j} V_{ij} u_i v_i u_j v_j + \sum_i V_{ii} v_i^2 \quad (5)$$

where V_{ij} are the matrix elements of the pairing interaction, Eq. (2), namely

$$V_{ij} = V_0 \int d^3r |\phi_i(\mathbf{r})|^2 |\phi_j(\mathbf{r})|^2 g_\tau[\rho(\mathbf{r}), \beta(\mathbf{r}) \tau_z],$$

where $\rho(\mathbf{r}) = \sum_i v_i^2 |\phi_i(\mathbf{r})|^2$.

After determining the single-particle energies of even-even nuclei, the odd-A nuclei are calculated with the so-called filling approximation for the odd particle starting from the HF+BCS solutions of neighboring even-even nuclei: one selects a pair of i and \bar{i} orbitals to be blocked,

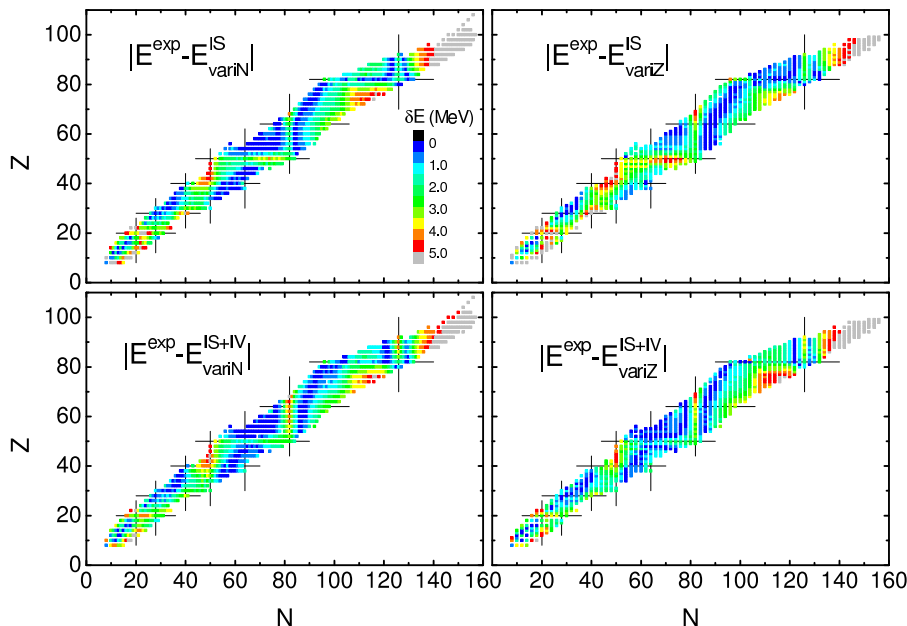


FIG. 2: (Color online) Binding energy differences between experimental data and calculations using the HF+BCS model with the IS and IS+IV pairing interactions. The left panels show the differences for even Z isotopes varying neutron numbers including both odd and even numbers. The right panel show those for even N isotones varying proton numbers including both odd and even numbers. The thin lines show the closed shells at $N(Z) = 20, 28, 40, 50, 64, 82$ and 126 . Experimental data are taken from Ref. [17]. See the text for details.

and changes the BCS parameters v_i^2 and v_i^2 for these orbitals. The change is to set $v_i^2 = v_i^2 = 1/2$ in Eq. (5) for the pairing energy at an orbital near the Fermi energy. Note that this approximation gives equal occupation numbers to both time-reversed partners, and does not account for the effects of time-odd fields. More details of the procedure are presented in Ref. [12].

The effect of time-odd HF fields on the mass were studied in Refs. [15, 16]. It was pointed out that the effect of the time-odd fields is of the order of 100 keV for the binding energy depending strongly on the configuration of the last particle, and does not show any clear sign of isospin dependence. Thus the time-odd field might not change conclusions of the present study in the following, while quantitative accuracy might need some fine tuning of the pairing parameters.

For the pairing channels we have taken the surface-type contact interaction, Eq. (4), and the isospin dependent interaction, Eq. (3). The density dependence of the latter one is essentially the mixed-type interaction between the surface and the volume types. The pairing strength V_0 depends on the energy window adopted for BCS calculations. The odd nucleus is treated in the filling approximation, by blocking one of the orbitals. The blocking candidates are chosen within an energy window of 10 MeV around the Fermi energy. This energy window is rather small, but it is the maximum allowed by the program EV8odd. It is shown that the BCS model used in the EV8odd code gives almost equivalent results

to the HF+Bogoliubov model with a larger energy window, except for unstable nuclei very close to the neutron drip line [12]. The pairing strengths V_0 for IS and IS+IV pairing interactions are adjusted to give the best fit to odd-even staggering of nuclear masses in a wide region of the mass table.

III. NUMERICAL RESULTS

A. Global data on odd-even staggering

The results for the mean square deviation of our global mass table calculations are shown in Fig. 1. Table I gives the values V_0 in Eq. (2) and the parameters for g_r and g_s is Eqs. (3) and (4) used in the present work. Optimal pairing strength values were found to be different for isotones (varying Z , constant N) and for isotopes (varying N , constant Z).

Figure 1 shows the mean square deviation σ of OES between experimental data and the HF+BCS calculations. The mean square deviation σ is defined as

$$\sigma = \sqrt{\sum_{i=1}^{N_i} |\Delta_i^{(3)}(HF + BCS) - \Delta_i^{(3)}(exp)|^2 / N_i} \quad (6)$$

where N_i is the number of data points. For the IS interaction, the results for neutrons show a shallow minimum at $V_0 \sim (1100 - 1300) \text{ MeV}\cdot\text{fm}^3$. For protons, the minimum

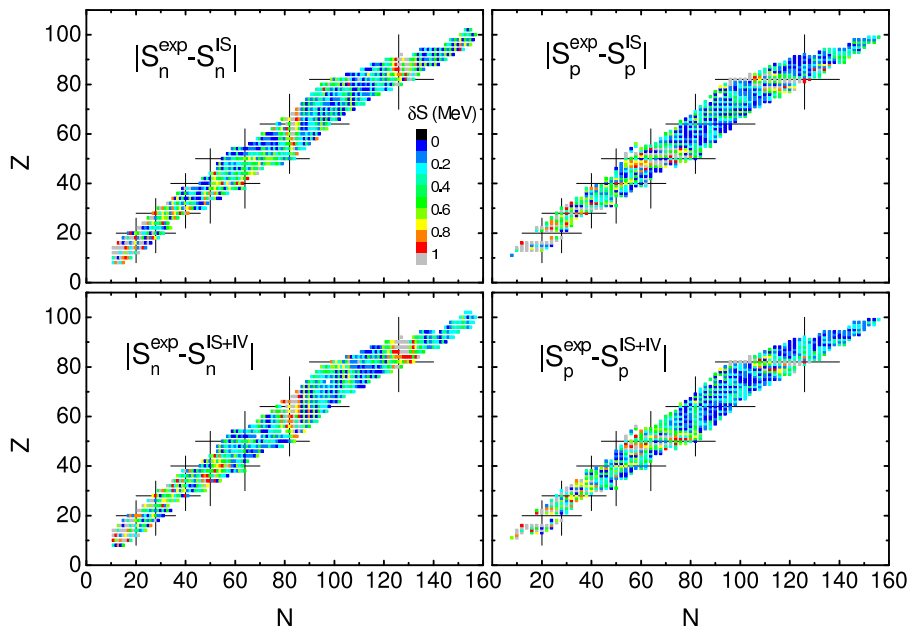


FIG. 3: (Color online) The same as Fig. 2 but for neutron and proton separation energies. See the caption to Fig. 2 and the text for details.

becomes at around $V_0 \sim 1500 \text{ MeV}\cdot\text{fm}^3$. This difference makes it difficult to determine a unique pairing strength common for both neutrons and protons. The results of IS+IV pairing show a minimum at $V_0 \sim 1100 \text{ MeV}\cdot\text{fm}^3$ for both neutron and proton OES which makes it easier to determine the value for the pairing strength. Adopted values for the following calculations are listed in Table I.

The systematic study of HF+BCS calculations are performed for various isotopes and isotones for all available data sets with ($Z = 8, \dots, 102$) and ($N = 8, \dots, 156$), respectively. Binding energy differences between experimental data and HF+BCS

$$\delta E = |E^{exp} - E^{cal}| \quad (7)$$

are shown for both IS and IS+IV pairing interactions in Fig. 2. The left panels show the values δE varying neutron numbers (including both odd and even numbers) for each even Z . The right panels show the values δE varying proton numbers (including both odd and even numbers) for each even N . With IS pairing, we can see a rather large deviation for $Z = 50$ isotopes in the upper right panel. This difference disappears in the case of IS+IV pairing shown in the lower right panel. On the other hand, for the $N = 82$ nuclei, the IS+IV interaction does not work that well. As far as the binding energies are concerned, the best results with IS+IV interaction are obtained for nuclei with $N = 60 - 78$ and $N = 86 - 96$.

Separation energy differences between experimental data and HF+BCS for protons and neutrons are plotted in Fig. 3. The HF+BCS results of neutron separation energies S_n are reasonable for medium and heavy mass nuclei with $N = 60 - 120$, except near the closed shell

$N = 82$. For heavy nuclei with $N = 126$, the calculated results are poorer than in other mass regions. For proton separation energy S_p , the HF+BCS also gives reasonable results, except in the $Z = 50$ and 82 mass regions.

In order to see the different outcomes between IS and IS+IV pairing interactions, the HF+BCS model calculations are shown together with empirical data in Fig. 4. In most of cases, the difference between the two pairing interactions are small. However, we can see a clear improvement of the agreement of S_p with empirical data of $N = 136$ isotones with IS+IV pairing in Fig. 5.

The differences of neutron OES Δ_n and proton OES Δ_p between HF+BCS and empirical data are shown in Fig. 6 for both IS and IS+IV pairing, respectively, in the upper and lower panels. The agreement between HF+BCS and the empirical data are good in the overall mass region except for masses with $Z = 50$ and at a small mass region $A < 60$. To clarify the difference between IS and IS+IV pairing, the OES differences Δ_n are shown in the upper panel of Fig. 7 for $Z = 52, 78$ and 92 isotopes. The HF+BCS results are compared with the experimental data and also the phenomenological parameterization based on liquid drop model,

$$\bar{\Delta} = c/A^\alpha \quad (8)$$

with $c = 4.66(4.31) \text{ MeV}$ for neutrons (protons) and $\alpha = 0.31$ which gives the rms residual of 0.25 MeV [12]. We can see clearly a better agreement of IS+IV results with empirical data for all isotopes. In the lower panel of Fig. 7, the OES differences Δ_n are shown for $N = 76, 102$ and 112 isotones. The results with IS+IV pairing certainly improve systematically the agreement with em-

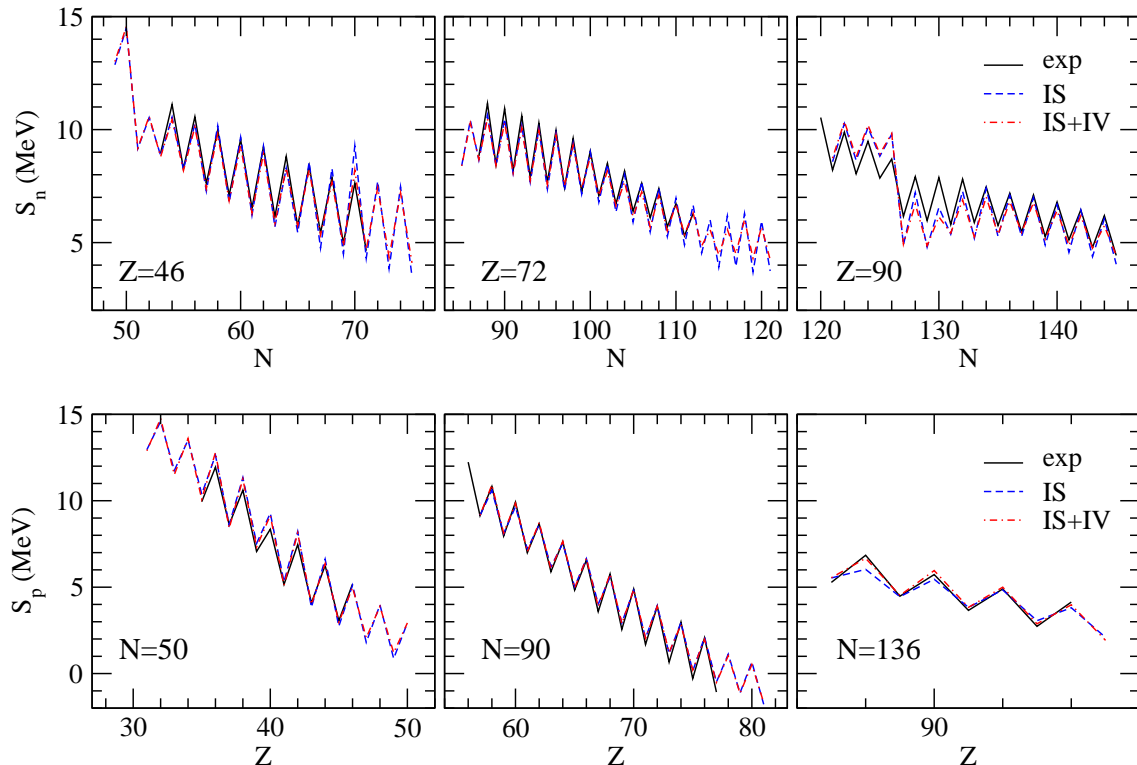


FIG. 4: (Color online) Neutron separation energies S_n of three isotope chains with $Z = 46, 72$ and 90 calculated by IS and IS+IV interactions in HF+BCS model (upper panels). The lower panels show the proton separation energies S_p for $N = 50, 90$ and 136 isotones. Experimental data are taken from Ref. [17]. See the text for details.

pirical data, especially for $N = 102$ isotones. The large increase of the HF+BCS model results at $Z = 81$ is an artifact due to the shell closure at $Z = 82$. It is interesting to notice that the liquid drop formula gives smooth mass number dependence which reflects well that of very heavy isotones with $N = 112$.

The average gaps $\Delta^{(3)}$ are tabulated for high and low isospins in Table II. Each isotope (isotone) in Fig. 7 is divided into two subsets of almost equal numbers of nuclei by a cut at some value of $I = (N - Z)/A$. Both the average proton and neutron $\Delta^{(3)}$ show smaller values for higher isospin so that the pairing interaction is weaker for neutron-rich nuclei. The IS+IV interaction reproduces properly the difference of the neutron $\Delta^{(3)}$ between high and low isospin nuclei. For proton $\Delta^{(3)}$ also, the IS+IV pairing gives a good account of the isospin effect than the IS pairing.

B. Nuclear radii

Nuclear radii provide basic and important information for various aspect of nuclear structure problems. The proton radii, or equivalently the charge radii with the correction of finite proton size, can be determined accurately by electron scattering and muon scattering experiments. However it is difficult to determine the neutron

radii of finite nuclei with the same accuracy level as that of the proton radii while there were several experimental attempts to determine the difference of the neutron to proton radius [19–21]. It should be noticed that the difference of the neutron and proton radii, $\delta r_{np} = r_n - r_p$, is called the neutron skin. It is thought that δr_{np} can give important constrains on the effective interactions used in nuclear structure study [22].

The neutron and proton radii of various isotopes and isotones are calculated by using the HF+BCS model with the two pairing interactions, IS and IS+IV. The results of neutron radii are shown in the left panel of Fig. 8. Since we do not find any appreciable differences between the two pairing interactions in the results, the results of IS+IV interactions will be mainly discussed hereafter. The results obtained by a simple empirical formula $r_n = r_0 N^{1/3}$ with $r_0 = 1.139$ fm [18] are also plotted in the figure. In general, the simple formula for r_n agrees well with the HF+BCS results. It is noticed that the HF+BCS model gives larger neutron radii for nuclei with $N < 40$ than the simple formula but smaller for nuclei with $N > 120$. The proton radii for $N = 20, 28, 40, 50, 82$ and 126 isotones are shown as a function of proton number Z in the right panel. The simple $Z^{1/3}$ dependence is also plotted to follow the formula $r_p = 1.263/Z^{1/3}$. The simple formula in general gives a good account of the HF+BCS data and could be a good

TABLE II: Average $\Delta^{(3)}$ for low isospin and high isospin nuclei and its difference. See the text for details.

	Data set		Low isospin	High isospin	Difference
Neutrons	$Z = 52$	Exp	1.36	1.08	-0.28
		IS	1.52	1.41	-0.11
		IS+IV	1.40	1.19	-0.21
	$Z = 78$	Exp	1.13	0.99	-0.14
		IS	0.96	1.16	0.20
		IS+IV	0.87	0.91	0.04
	$Z = 92$	Exp	0.77	0.56	-0.21
		IS	0.90	0.80	-0.10
		IS+IV	0.70	0.55	-0.15
Protons	$N = 76$	Exp	1.19	0.93	-0.26
		IS	1.13	0.87	-0.26
		IS+IV	1.13	0.98	-0.15
	$N = 102$	Exp	0.96	0.63	-0.33
		IS	0.79	0.39	-0.40
		IS+IV	0.92	0.59	-0.33
	$Z = 112$	Exp	0.87	0.66	-0.21
		IS	0.58	0.61	0.03
		IS+IV	0.67	0.70	0.03

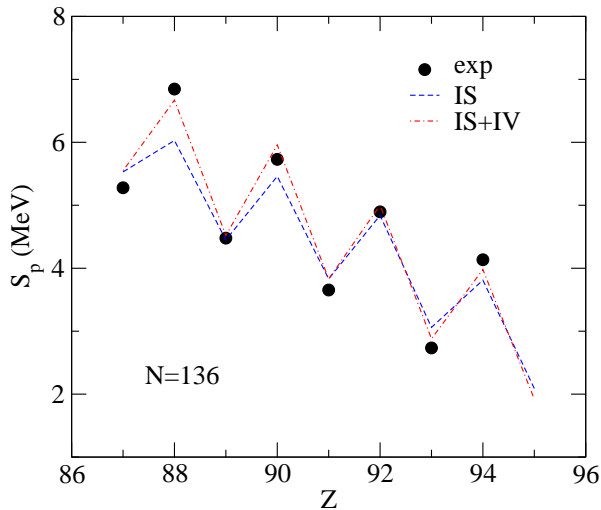


FIG. 5: (Color online) Proton separation energies S_p of $N = 136$ isotones calculated by IS and IS+IV interactions in HF+BCS model. Experimental data are taken from Ref. [17]. See the text for details.

starting point for describing the isospin dependence of nuclear charge radii. However we can see some deviation between the HF+BCS and the simple formula especially heavy $N = 50$ and $N = 82$ isotones.

The neutron skin $r_n - r_p$ calculated by HF+BCS model with the two pairing interactions are shown in Fig. 9. The neutron skin becomes as large as 0.4 fm near the neutron drip line with $Z < 28$. On the other hand, the neutron skin is at most 0.25 fm in neutron-rich nuclei with $Z > 50$. For proton-rich nuclei, the proton skin becomes 0.1 fm with $Z < 56$ and smaller than 0.05 fm

in heavier isotopes, larger than $Z = 56$. The results of IS and IS+IV pairings are shown in the left panel and right panel, respectively. In general, the two pairing interactions give almost the same results as shown in Fig. 9. However, it is noticed that the IS+IV pairing gives somewhat smaller neutron skins than the IS pairing in very neutron-rich nuclei such as ^{136}Sn , ^{150}Ba and ^{218}Po . The calculated values are compared with empirical data of Sn isotopes obtained from studies of spin-dipole resonances [19] and antiprotonic atoms [20] in the left panel Fig. 10. The calculated values show reasonable agreement with the empirical data within the experimental error. The isospin dependence of neutron skin is shown in the right panel of Fig. 10 together with empirical values obtained by antiprotonic atom experiments in a wide range of nuclei from ^{40}Ca to ^{238}U . The slope of experimental data as a function of the isospin parameter $I = (N - Z)/A$ is reproduced well by our calculations.

The neutron skin of ^{208}Pb has been discussed intensively in relation with neutron matter properties. The systematic studies of scattering data yield the empirical value $r_n - r_p = 0.17 \pm 0.02$ fm which is close to another empirical value $r_n - r_p = 0.15 \pm 0.02$ fm from the study of antiprotonic-atom systems. The model independent determination of parity violation experiment at Jefferson Laboratory [22] has been proposed and performed recently to obtain the neutron skin of ^{208}Pb . However the statistics was poor and needs improvement by more data accumulation. Our calculated value $r_n - r_p = 0.157$ fm is close to the experimental values by the two systematic studies.

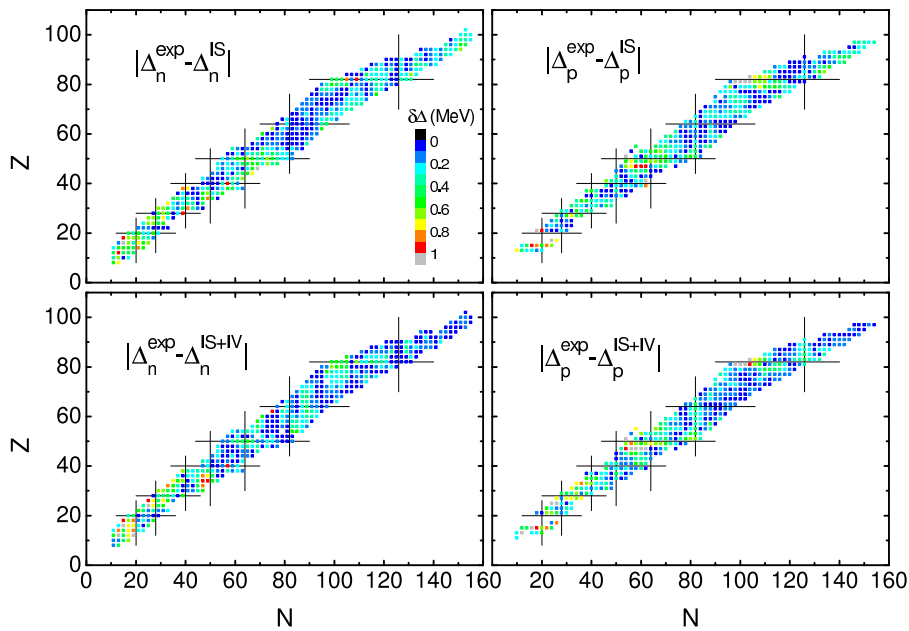


FIG. 6: (Color online) The same as in Fig. 2 but for OES for neutrons and protons. See the caption to Fig. 2 and the text for details.

IV. SUMMARY AND CONCLUSIONS

In summary, we studied the binding energies, separation energies and OES by using HF+BCS model with SLy4 interactions together with the isospin dependence pairing (IS+IV pairing) and isoscalar (IS pairing) interactions. The calculations are performed with the EV8odd code for even-even nuclei and also even-odd nuclei using the filling approximation. For the neutron pairing gaps, the IS+IV pairing strength decreases gradually as a function of the asymmetry parameter $(\rho_n(r) - \rho_p(r))/\rho(r)$. On the other hand, the pairing strength for protons increases for larger values of the asymmetry parameter because of the isospin factor in Eq. (3). The empirical isotope dependence of the neutron OES, $\Delta_n^{(3)}$, is well reproduced by the present calculations with the isospin dependent pairing compared with the IS pairing. We can also obtain a good agreement between the experimental proton OES and the calculations with the isospin dependent pairing for $N = 50$ and $N = 82$ isotones.

The neutron and proton radii were also studied by using the same HF+BCS model with the two pairing interactions. The two pairing interactions give essentially the same results for the radii except for a few very neutron-rich nuclei. We found systematically large neutron skins

in very neutron-rich nuclei with $|r_n - r_p| \sim 0.4$ fm, while the proton skin is rather small even in nuclei close to the proton drip line because of the Coulomb interaction. The calculated results of neutron skin show reasonable agreement with the empirical data including the $(N - Z)$ dependence of the data.

We tested the IS+IV pairing for the Skyrme interaction SLy4 and found the results reproduce well the systematical experimental data. Thus, we confirm a clear manifestation of the isospin dependence of the pairing interaction in the OES in comparison with the experimental data both for protons and neutrons.

Acknowledgments

This work was partially supported by the U.S. DOE grants DE-FG02-08ER41533 and DE-FC02-07ER41457 (UNEDF, SciDAC-2), the Research Corporation, and the JUSTIPEN/DOE grant DEFG02-06ER41407, and by the Japanese Ministry of Education, Culture, Sports, Science and Technology by Grant-in-Aid for Scientific Research under the Program number C(2) 20540277. Computations were carried out on the XT4 Jaguar supercomputer at the Oak Ridge National Laboratory.

[1] A. Bohr, B. R. Mottelson, and D. Pines, Phys. Rev. **110**, 936 (1958).

[2] A. Bohr and B. R. Mottelson, “Nuclear Structure” (Benjamin, New York, 1969) Vol. I.

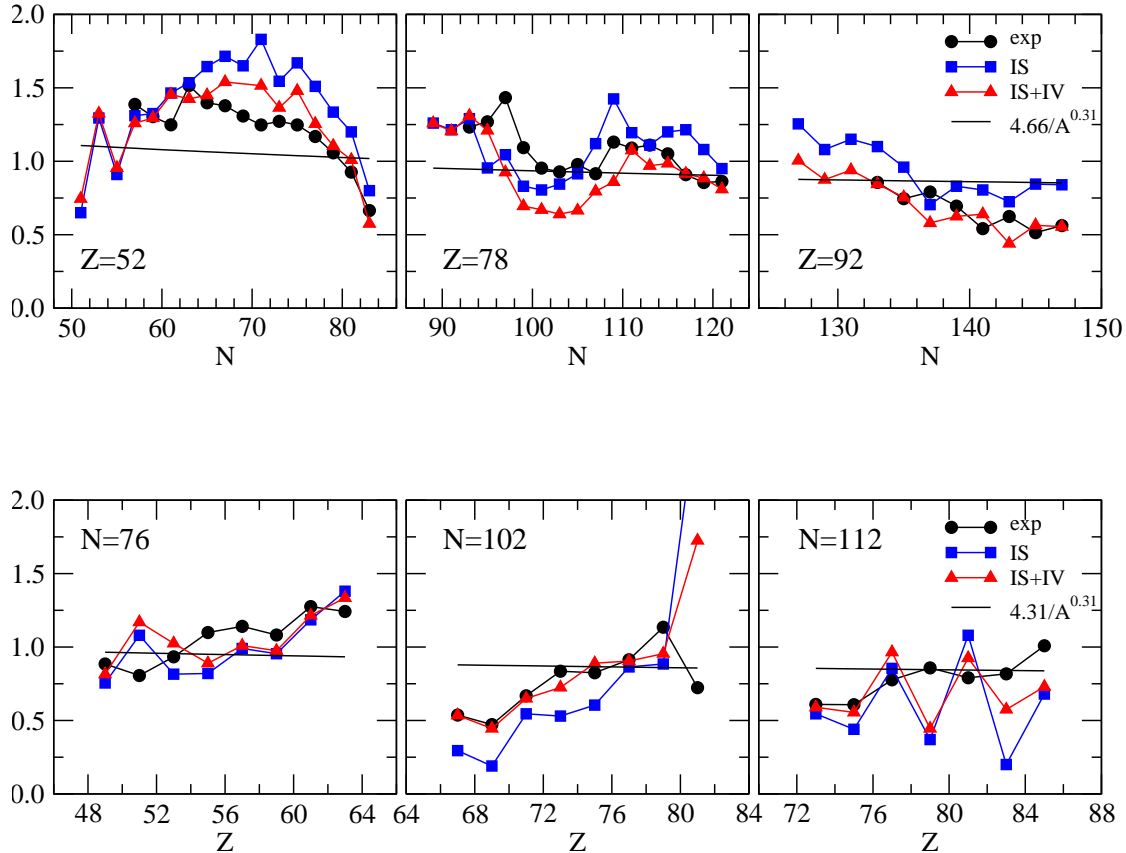


FIG. 7: (Color online) The neutron and proton OES, Δ_n and Δ_p , calculated with the HF+BCS model with IS and IS+IV interactions. Experimental data are taken from Ref. [17]. See the text for details.

- [3] D. M. Brink and R. Broglia, “Nuclear Superfluidity, Pairing in Finite Systems”, Cambridge Monographs on Particle Physics, Nuclear Physics and Cosmology, vol 24 (2005).
- [4] M. Bender, P.-H. Heenen and P.-G. Reinhard, Rev. Mod. Phys. **75**, 121 (2003).
- [5] M. V. Stoitsov, J. Dobaczewski, W. Nazarewicz and P. Borycki, Int. J. Mass Spectrum, **251**, 243 (2006).
- [6] W. Satula, J. Dobaczewski and W. Nazarewicz, Phys. Rev. Lett. **81**, 3599 (1998).
- [7] T. Duguet, P. Bonche, P.-H. Heenen, and J. Meyer, Phys. Rev. C **65**, 014311 (2001).
- [8] J. Margueron, H. Sagawa and K. Hagino, Phys. Rev. C **76**, 064316 (2007).
- [9] M. Yamagami and Y. R. Shimizu, Phys. Rev. C **77**, 064319 (2008).
- [10] P. Bonche, H. Flocard and P. H. Heenen, Comput. Phys. Commun. **171**, 49 (2005).
- [11] G. Bertsch and C.A. Bertulani, unpublished. EV8odd code available upon request.
- [12] G. F. Bertsch, C. A. Bertulani, W. Nazarewicz, N. Schunck and M. V. Stoitsov, Phys. Rev. C **79**, 034306 (2009).
- [13] C.A. Bertulani, Hongfeng Lu, H. Sagawa, Phys. Rev. C **80**, 027303 (2009).
- [14] “The Universal Nuclear Energy Density Functional”, a SciDAC project. URL: <http://unedf.org>
- [15] T. Duguet, P. Bonche, P. H. Heenen and J. Meyer, Phys. Rev. C **65**, 014310 (2001);
- [16] J. Margueron, M. Grasso, G. Colò, S. Goriely and H. Sagawa, J. of Phys. G **36**, 125103 (2009).
- [17] G. Audi, A. H. Wapstra and C. Thibault, Nucl. Phys. **A729**, 337 (2003).
- [18] Jie Meng et al., Prog. Part. Nucl. Phys. **57**, 470 (2006).
- [19] A. Krasznahorkay et al, Phys. Rev. Lett. **82**, 3216 (1999).
- [20] A. Trzcinska et al., Phys. Rev. Lett. **87**, 082501 (2001).
- [21] J. Jastrzebski et al, Int. J. Mod. Phys. E **13**, 34 (2004).
- [22] C. J. Horowitz and J. Piekarewicz, Phys. Rev. C **64**, 062802, (2001).

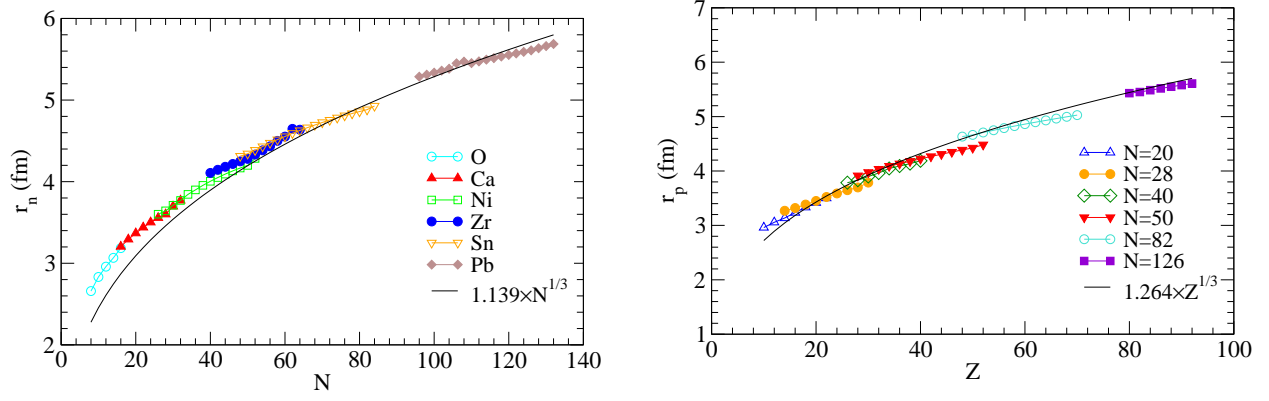


FIG. 8: (Color online) Neutron and proton radii of various isotopes and isotones calculated by means of the HF+BCS model with IS+IV interaction. The solid lines are empirical fits used in Ref. [18]. See the text for details.

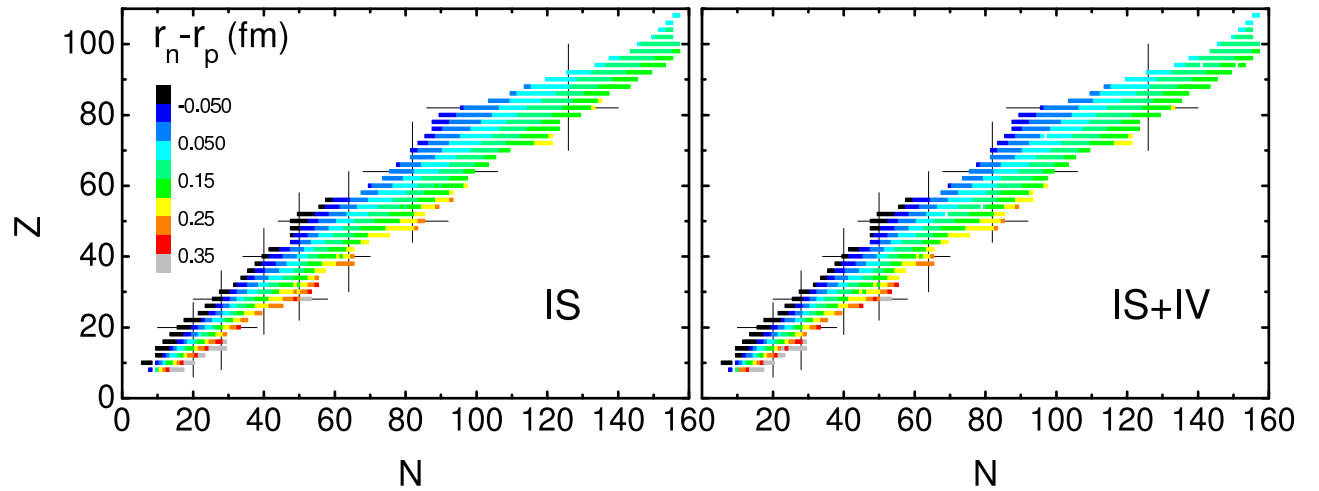


FIG. 9: (Color online) Neutron skin thickness for isotopes and isotones calculated by means of the HF+BCS model with IS and IS+IV interactions. The thin lines indicate the closed shells with N (or Z)=20, 28, 40, 50, 64, 82 and 126. See the text for details.

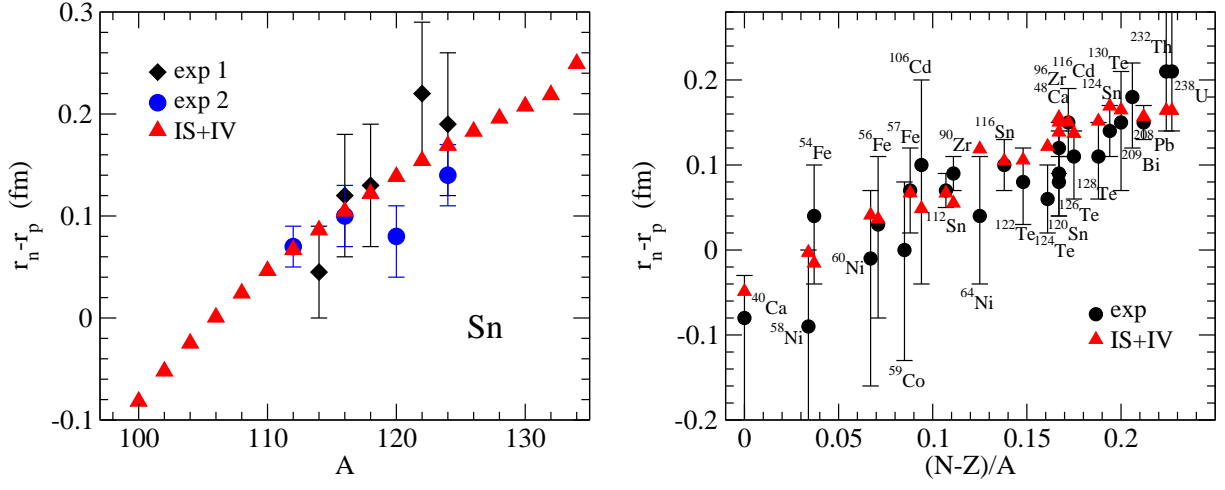


FIG. 10: (Color online) *Left* - Neutron skin for Sn isotopes obtained with the HF+BCS model with IS+IV interaction. Experimental data are taken from Ref. [19, 20]. *Right* - Neutron skin as a function of isospin parameter $I = (N - Z)/A$ calculated by means of the HF+BCS model with IS+IV interaction. Experimental data are taken from Ref. [21]. See the text for details.